Spatial arrangement of casein micelles and whey protein aggregate in acid gels: Insight on mechanisms

Robi Andoyo, Fanny Guyomarc'H, Agnès Burel, Marie-Hélène Famelart

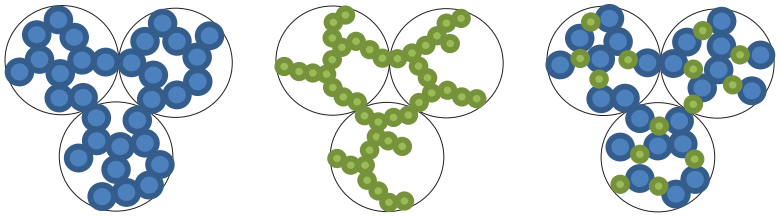

Casein micelles

Whey protein aggregates

Mixture

Spatial arrangement of casein micelles and whey protein aggregate in acid gels: Insight on mechanisms

Robi ANDOYO[abc], Fanny GUYOMARC'H[ab], Agnes BUREL[d],

Marie-Hélène FAMELART[ab,*]

[a]INRA, UMR1253, Science et Technologie du Lait et de l'Œuf, 65 rue de St Brieuc, F-35 042 Rennes cedex, France

[b]AGROCAMPUS OUEST, UMR 1253, Science et Technologie du Lait et de l'Œuf, 65 rue de St Brieuc, F-35 042 Rennes cedex, France

[c]Faculty of Agriculture Industrial Technology, Padjadjaran University, Indonesia

[d]Université de Rennes 1 France, Microscopy Rennes Imaging Center of SFR BIOSIT. 2 Avenue du professeur Léon Bernard, 35043 Rennes cedex, France

* Corresponding author; Tel: +33.223.48.53.43; Fax: +33.223.48.53.50; email address: marie-helene.famelart@rennes.inra.fr

Keywords: whey proteins, casein micelles, acid gel, rheology, microstructure, fractal analysis

Running title: mechanism of acid gelation of model acid gels

ABSTRACT

Skim milk used for the yoghurt manufacture contains 2 main colloidal particles, the native micellar casein (NMC) and the heat-induced whey protein aggregates (WPA). The aim of this study was to understand how these 2 colloids organize in space to form binary acid gels. While acid milk gels were considered homogeneous for scales typically above ~10 µm, shorter length scales were examined to investigate the early stages of particle aggregation. The NMC and WPA were dispersed in milk permeate at different protein concentrations,

separately or in an 80/20 w/w mixture (MIX). Acidification was performed at 35 °C with glucono-δ-lactone to achieve a final pH at ~ 4.5 in 6 h. Acid gelation was studied by rheology, while the microstructure of the gels at pH 4.5 was studied by confocal scanning laser microscopy and transmission electron microscopy (TEM). Using Shih et al.'s (1990) model on the rheological data, it seemed that aggregation in the NMC and MIX mixtures was driven by the casein micelles and therefore differed from that of the WPA suspension. The different organizations were confirmed using image analysis of confocal or TEM images. The differences in gel formation were discussed in terms of the different interactive properties of the surface of these 2 colloids, together with their different internal structure.

1. Introduction

The protein components of milk contain two types of colloidal particles, namely caseins and whey proteins. Caseins assemble as colloidal particles having diameter of ~ 200 nm called casein micelles that occupy a volume fraction Φ of ~0.1 in skim milk (Holt, 1992). These micelles contain several thousands of α_{s1}, α_{s2}, β- and κ-casein molecules as well as minerals, essentially in the form of colloidal calcium phosphate (CCP) (de Kruif, 1999; Fox & Brodkorb, 2008). CCP ionic bridges and hydrophobic interactions are responsible for the integrity of the micelles (Dalgleish, 2011; Horne, 1998). The κ-casein, located at the surface of casein micelles, contributes to their stability through steric and electro-negative repulsion (de Kruif & Huppertz, 2012; Panouillé, Durand, Nicolai, Larquet, & Boisset, 2005). During acidification, the hairy layer of κ-casein collapses at pH ~6.0 while the electrostatic repulsion decreases as the casein micelles reach their isoelectric pH (pI) of about 4.6, where destabilization eventually occurs (Lucey & Singh, 1998).

Heating of milk at ~60°C or above makes the whey protein unfold and irreversibly denature, yielding to the formation of heat-induced whey protein aggregates (WPA), built through thiol oxidation, thiol/disulphide exchange and hydrophobic interactions (Donato & Guyomarc'h, 2009; Parris, Anema, Singh, & Creamer, 1993; Parris, Hollar, Hsieh, & Cockley, 1997; Singh & Creamer, 1991). Upon acidification, these aggregates accelerate the destabilization of casein micelles due to their higher surface hydrophobicity and slightly higher pI (Guyomarc'h, Renan, Chatriot, Gamerre, & Famelart, 2007; Morand, Dekkari, Guyomarc'h, & Famelart, 2012; Morand, Guyomarc'h, Legland, & Famelart, 2012). Aggregates are also thought to act as bridges between the casein micelles and to strengthen the acid gel network (Alexander, Corredig, & Dalgleish, 2006; Famelart, Tomazewski, Piot, & Pezennec, 2004; Guyomarc'h, Queguiner, Law, Horne, & Dalgleish, 2003). Andoyo et al. (2014) showed that the coating of only ~8% of the casein micelle surface by WPA produced

gels with significantly higher storage modulus values (G') than those made of casein only. Therefore, the interaction between these particles and the mechanism of their assembly is likely to direct the structural and mechanical properties of the acid gel. However, the mechanisms that drive this interaction need to be further investigated.

Acid milk gels are particulate gels that appear as a porous, homogeneous material at length scales above tens of μm. Various models have been proposed to describe their formation and structure; namely the adhesive sphere, the percolation and the fractal models (Horne, 1999). While the adhesive sphere theory tells whether particles are stable in certain environmental conditions, the percolation theory informs on the dynamics of gel formation from the point when diffusion in the bulk is restricted by the growth of flocs of aggregated particles. In other words, the former rather focuses on the initial stages of aggregation at the particle's length scale, while the latter rather applies from the gelation point on ward and at length scales of tens of μm and beyond. At intermediate length scales, typically 0.1-5 μm, Bremer et al. (1989) applied the self-similarity concept to describe the acid gelation of casein particles. Therefore, it is proposed that the fractal model may describe particle aggregation in a mixture of both particles, from the point when acidification render the particles reactive (de Kruif, 1999) to the point when clusters have grown enough to come in close contact, interpenetrate and percolate. To the authors' knowledge, little research has yet been undertaken that could help model early flocculation in binary colloidal suspensions of casein micelles and whey protein aggregates, where the two particles differ in size and reactivity (Andoyo et al., 2014; Nair, Dalgleish, & Corredig, 2013).

Various scaling models have been developed and used in protein and colloidal gels to infer information on the mechanism of assembly of particles and on the structure of the final particulate gel network from rheological data or image analysis (Alting, Hamer, de Kruif, & Visschers, 2003; Bremer, Bijsterbosch, Schrijvers, Van Vliet, & Walstra, 1990; Buscall,

Mills, Goodwin,& Lawson, 1988; Marangoni, Barbut, McGauley, Marcone, & Narine, 2000; Shih, Shih, Kim, Liu, & Aksay, 1990; Sonntag & Russel, 1987). In this approach, the fractal dimension (D_f) is used to describe the occupancy of the structure in the volume of the gel, while the scaling behavior can give insight on the mechanism of assembly of the particles. The model developed by Shih et al. (1990) proposes an estimation of the fractal dimension (D_f) based on the rheological properties of the gel system. This model calculates the D_f values using G' and the strain at limit of linearity (γ_0) of gels produced at different protein concentrations (C). Furthermore, this concept gives insight to the building of the gel, since aggregation can follow two distinct pathways indicated by the either positive or negative slope of $\log(\gamma_0)$ as a function of $\log(C)$.

In this study, the gelation properties, aggregation behavior and the fractal dimension of the flocs of casein micelles, of the WPA and of their mixture in acid gel were investigated, in order to better understand the mechanisms of formation of dairy acid gels. Since milk is a rather crowded system, diffusion is probably rapidly restricted upon cluster growth and fractal structures may be searched only locally. For that reason, microscopies were also used to support the rheological approach.

2. Materials and Methods

2.1. Materials

A commercial whey protein isolate (WPI) (Prolacta 95, Lactalis Ingredients, Bourgbarré, France) was used as the source of protein in this study. The protein content of the WPI powder is ~939 gkg^{-1} dry matters. Protein content was determined by Kjeldahl method (conversion factor 6.38).

Native micellar casein (NMC) was prepared by microfiltration of raw skim milk, diafiltration and spray-drying as described by Schuck et al. (1994). Skim milk microfiltration

106 also yielded a whey protein permeate that was further ultra-filtered to produce milk
107 ultrafiltration permeate (MUF). The MUF was stored at 5°C after addition of 0.2 g L^{-1} sodium
108 azide (NaN_3). All other reagents were of analytical grade.

109 ***2.2 . Preparation of the model systems***

110 WPA was produced by heating an aqueous WPI solution at total protein concentration of
111 90 g $kg^{-1}$and pH 7.5 at 68.5 °C for 2 h as described by Vasbinder, van de Velde and de Kruif
112 (2004) and as used in Andoyo et al. (2014). The protein content of the resulting WPA
113 suspension was determined spectrophotometrically using absorbance at 280 nm and an
114 experimental extinction coefficient value of 1.2244 L g^{-1} cm^{-1} (Morand, Guyomarc'h,
115 Pezennec, & Famelart, 2011). WPA was then standardized at 70 g kg^{-1} total protein using
116 MUF, extensively dialyzed (6-8 molecular-weight cut-off Spectra Por membrane) against
117 commercial ultra-high temperature (UHT) skim milk to fully replace the solvent phase by
118 MUF, then diluted again with MUF to reach concentrations (*C*) ranging 14 g kg^{-1} to 62 g kg^{-1}.
119 Considering a voluminosity of 5.512 mL g^{-1} for the WPA particles as measured at 20°C and
120 pH 6.6 (Andoyo et al., 2014), the corresponding volume fractions ranged from 8 to 35% (v/v).
121 This value of the volume fraction is only a rough estimate as we have no idea of the changes
122 in voluminosity of WPA with temperature and pH.

123 A mother suspension of NMC at total protein concentration of 105 g kg^{-1} was produced by
124 gradually dispersing the required amount of NMC powder in MUF at 40°C with gentle
125 stirring for 4 hours. The suspension was stored overnight at 4°C for complete hydration
126 before further processing. NMC suspension at different total protein concentrations were
127 prepared by diluting mother suspension with MUF. Total protein concentration of NMC
128 ranged from 42g kg^{-1} to 98g kg^{-1}. Considering a voluminosity of 4.752 mL g^{-1} for the NMC
129 particles as measured at 20°C and pH 6.6 (Andoyo et al., 2014), a 10% decrease of the
130 voluminosity with the increase in temperature from 20 to 35°C (Noebel, Weidendorfer, &

Hinrichs, 2012) and a 4%and 32% decrease in voluminosity with the decrease in pH from 6.6 to 5.6 or 6.6 to 4.8, respectively (van Hooydonk, Hagedoorn, & Boerrigter, 1986), the corresponding volume fractions ranged approximately from 12 to 42% (v/v). The values of pH 5.6 and 4.8 are the respective pH of gelation of the suspensions at high and low concentration where the volume fraction has to be calculated. Using the same method, the volume fractions for the MIX systems were 6 to 37%.

Mother mixtures of NMC and WPA at 90 g kg^{-1} and at the weight ratio of 80/20 were prepared by mixing appropriate amounts of each mother suspension. The mother mixture (MIX) suspension was then diluted with MUF to prepare mixtures ranging from 15 g kg^{-1} to 90 g kg^{-1} total protein concentration (Table 1).

Systems will be called e.g. NMC45 or WPA15 or MIX60, the number representing their approximate total protein concentration in g kg^{-1} (Table 1). All dairy systems were replicated at least two times and analyzed within one week.

2.3. Characterization of particles: Isoelectric pH

The apparent isoelectric pH (pI) of the WPA and NMC were determined using interpolation to 0 of the experimental measurement of the electrophoretic mobility (in µm cm V^{-1} s^{-1}), while the pH of the MUF was varied from 2.5 to 6.5 using HCl. The electrophoretic mobility was measured at 50 V and at 20°C on a Zetasizer nano ZS equipment (λ = 633 nm, Malvern Instruments, Orsay, France). Colloidal suspensions were diluted at least 1:10 v/v in the MUF (dielectric constant 80.4, viscosity 1.1454 mPas, refractive index 1.337). This method yields lower apparent pI values (by ~0.2 pH units) than those obtained with MUF extracted from acidified skim milk (Guyomarc'h et al., 2007) or acidified MUF with added calcium (Morand et al., 2011), where the solubilization of CCP is taken into account. The resulting values were used only for comparison.

2.4. Rheological measurements

The WPA, NMC and MIX suspensions at different concentrations were equilibrated at 35°C then acidified at this temperature using addition of glucono-δ-lactone (GDL) as to achieve a final pH value of 4.5 within 6 h (See concentrations of GDL used in Table 1).

Formation of the gels was monitored through the measurement of the storage modulus, G' (in Pa), upon acidification at 35° C using an AR2000 rheometer (TA Instruments, Guyancourt, France) equipped with a cone-plane geometry (diameter 6 cm and cone angle 4°) using the oscillatory mode at a frequency of 1 Hz and 0.1% strain. The GDL was added to the sample, stirred for 1 min and the dairy system was then transferred to the rheometer. Low density paraffin oil was added around the sample to prevent evaporation. The gelation pH was defined as the moment when G' > 1 Pa, while the storage modulus at pH 4.5 was considered to be the final G' at 35 °C (G'_{max}).

The gels at pH 4.5 were eventually subjected to a flow test. The strain, γ (dimensionless), was progressively increased at a constant rate of $0.01 s^{-1}$ until the gel broke. From this, the strain at the limit of linearity (γ_0) or the end of the pure elastic behavior was obtained as the strain above which the slope of the stress versus strain curve decreased of 5% from its maximal value (insert Fig. 4). Each replicated system was measured twice.

2.5. Microstructure of acid gels

2.5.1. Confocal laser scanning microscopy (CLSM)

Samples for confocal image measurements were prepared as described by Andoyo et al. (2014). Briefly, the dairy system suspensions at 35°C were labeled using 0.06 µL of rhodamine B isothiocyanate (RITC) per gram protein (from a 85 g L^{-1} RITC solution in dimethylsulfoxyde, Sigma-Aldrich, St Quentin Fallavier, France) and stirred for 15 min prior to the addition of GDL.

179 Immediately after GDL dispersion, ~60 µL of the labeled sample was deposited on a
180 conclave glass slide, covered with a cover slip, sealed with nail varnish and incubated at 35°C
181 until pH 4.5. The slides were then imaged at 543 nm using a TE2000-E Nikon C1i inverted
182 confocal laser scanning microscope (CLSM, Nikon, Champigny-sur-Marne, France). Each
183 image was digitized in grey levels as a 512 x 512 pixel matrix (127.3 x 127.3 μm^2).

184 *2.5.2. Transmission electron microscopy (TEM)*

185 The same procedure of microencapsulation as described in Andoyo et al. (2014) was
186 employed for sample preparation of the gels. Briefly, gels were formed at 35°C in capillary
187 tubes, fixed by glutaraldehyde-cacodylate and tannic acid-cacodylate solutions, dehydrated by
188 ethanol, then embedded in an Epon-Araldite-DMP30 resin polymerized at 60°C. Ultra-thin
189 sections (90 nm) of gels were cut in Leica UC6 ultra-microtome (Leica Microsystems,
190 Vienna) and stained with 40 g L^{-1} uranyl acetate for one hour.

191 The microencapsulation technique used in the current study has been used mainly for
192 TEM of suspensions and emulsions (Kalab, 1981), but more rarely for acid gels like yoghurts.
193 Most of the time, acid dairy gels are observed by scanning electron microscopy, with a
194 glutaraldehyde fixation or by using a cryo-step. This encapsulation technique avoids problems
195 for the sampling of soft gels and for the tendency of the gel to disperse into glutaraldehyde
196 during fixation, but there is still problems arising from the fixation with glutaraldehyde,
197 because of added intermolecular cross-links between proteins by the dialdehyde (Pawley,
198 2010).

199 Sections were viewed with a JEOL 1400 transmission electron microscope (JEOL,
200 Croissy-sur-Seine, France) supplied with GATAN Orius camera (Digital Micrograph
201 software).

202 ***2.6. Determination of an apparent fractal dimension***

2.6.1. From rheological measurement

An apparent fractal dimension (D_f) was evaluated from the slopes of the log (γ_0) against the log (C) and log (G') against log (C) based on the model of Shih et al. (1990) and using the following equations when the slope of log (γ_0) *versus* log (C) is negative (equation 1-2) or positive (equation 3-4) :

$$G' \propto C^{(3+x)/(3-D_f)} \quad (1)$$

$$\gamma_0 \propto C^{-(1+x)/(3-D_f)} \quad (2)$$

$$G' \propto C^{(1)/(3-D_f)} \quad (3)$$

$$\gamma_0 \propto C^{1/(3-D_f)} \quad (4)$$

With x, the backbone fractal dimension of the flocs, where the backbone is the fraction of the fractal structure that is implied in stress transmission and hence, in the rheological response of the structure (Genovese, 2012). Values from 1 to 1.3 are generally found for x (Shih et al., 1990). The link regime of the particle assemblies can be identified by plotting log γ_0 against the log C. Shih et al. (1990) established that γ_0 decreases with increasing C for a strong-link assembly, while it increases for weak-link. For the weak-link regime, apparent D_f was only calculated from G' values, while for the strong-link assembly, the apparent D_f values for $x = 1$ and 1.3 were calculated, respectively, as done in previous works (Hagiwara, Kumagai, & Nakamura, 1996; Ikeda, Foegeding, & Hagiwara, 1999; Shih et al., 1990).

2.6.2 From confocal image analysis

Images of the NMC, WPA and MIX gels were analysed with the public domain software ImageJ 1.45s (http://rsb.info.nih.gov/ij/) and the fractal count plug-in (http://www.pvv.org/~perchrh/imagej/fractal.html). The images were transformed into 8 bit grey scale binary images of 512 x 512 pixels and were then thresholded using the method of

Pugnaloni et al. (2005). In this method, model systems before gelation were imaged as homogeneous images of the proteins and their mean grey level was calculated (GL_M). Hence, if any pixel of an image of a gel has a grey level larger (i.e. whiter pixel) than the GL_M, it means that this pixel belongs to a structured place of the gel, namely to the network, and this pixel=1. Conversely if the pixel has a grey level lower than the GL_M (i.e. dark pixel), it belongs to the gel pores and the pixel=0. The apparent fractal dimension value (D_f) was then measured on the converted image using the box counting method (Kaye, 1994) as a widespread technique used for gel microstructure analysis (Awad, Rogers, & Marangoni, 2004; Bertoluzzo, Bertoluzzo, Luisetti, & Gatti, 1998; Bi, Li, Wang, & Adhikari, 2013; Eissa & Khan, 2005; Hagiwara, Kumagai, Matsunaga, & Nakamura, 1997; Kuhn, Cavallieri, & Da Cunha, 2010; Torres, Amigo Rubio, & Ipsen, 2012). The main principle of this method is to plot boxes of increasing sizes over an image and to count the number of boxes containing part of the protein network or flocs. The apparent fractal dimension value was calculated as the slope of the plot log number of boxes (N_ε) versus log size of the box (ε)or following this equation:

$$D = -\frac{\mathrm{Log}N_\varepsilon}{\mathrm{Log}\varepsilon} \quad (5)$$

The slope (D) represent the two-dimensional space fractal dimension, the 3-D apparent fractal dimension is calculated with the following equation:

$$D_f = D + 1 \quad (6)$$

2.6.3 From TEM image analysis

TEM images of the NMC, WPA and MIX gels were analyzed with the ImageJ as for the confocal image analysis. The images were automatically thresholded using the ImageJ isodata algorithm where a threshold T is iteratively shifted toward the maximal grey value of the image until the mean grey level of pixels having a grey level < T is close to the mean grey

level of the pixels having a grey level >T. The software then determined the area and perimeter of objects or flocs for each cross section of the gel network in the image. The two-dimensional apparent fractal dimension (*D*) for the flocs was calculated by regression analysis of the logarithm of their areas versus the logarithm of their corresponding perimeters (Dong, Wang, & Feng, 2011; Wang, Lu, Du, Shi, & Wang, 2009). The slope of the regression line is the value of *D*. The three-dimensional apparent fractal dimension (D_f) was calculated as in equation 6.

3. Results and discussion

In the current study, it is postulated that varying the concentration of any of the 3 systems only changed the number of particles, without affecting the properties of the colloids, such as their size, charge and isoelectric pH.

3.1. Acid gelation of the model systems

Using the different amounts of GDL as determined in Table 1, the kinetics of the pH versus acidification time were identical for all tested systems regardless of their total protein concentration or composition (results not shown). Noteworthy, what is important is the difference between the rate of the pH decrease and the rate of aggregation, which may affect gelation (Horne, 2001). Only when the aggregation rate can be shown to be identical for all systems or is much faster than the pH change, can the kinetics be fully ignored. Fig. 1A, 1C and 1E show the storage modulus (G') as a function of pH at different total protein concentrations of WPA, NMC or MIX systems, respectively. Increasing the total protein concentration in all systems resulted in an earlier gel formation, i.e. a higher pH of gelation, and led to a higher G' value at pH 4.5. The G' showed a steep increase from the point where the gels were formed (G'>1 Pa) then leveled off. However a G' plateau value was not reached within 6h of acidification (Van Vliet, Roefs, Zoon, & Walstra, 1989). A "G' shoulder" was observed for protein concentrations above 45 g kg^{-1} for the NMC system and above 15 g kg^{-1}

for the MIX system at pH 4.8-4.9 and then the G' value increased further until pH ~ 4.5. Fig. 1B, 1D and 1F show the value of tan δ as a function of pH of the model milk systems at different total protein concentrations. A higher value of tan δ indicates a more viscous-like behavior of the gel. For the WPA systems, the value of tan δ decreased as the gel formed, then leveled off towards a value of ~0.17. Meanwhile, for NMC and MIX systems, i.e.when casein micelles were present in the systems, the gels seemed to rearrange during acidification, as evidenced by the local maximum of tan δ at pH 4.9-5.1 (Fig.1D and 1F). This maximum in the loss tangent was related to the shoulder seen in the G' curves (Fig. 1C,E) and is due to the solubilization of the CCP from the micelles resulting in a transient loosening of the gel network (Anema, 2009; Lucey, 2002; Ozcan-Yilsay, Lee, Horne, & Lucey, 2007). The values of the pH at the $\tan\delta_{max}$ are plotted as a function of the casein concentration (Fig. 2). We must point up that for the MIX series, the increase in casein concentration was also correlated with an increase in the whey protein aggregate concentration. It was clear that the pH at tan δ_{max} decreased with increasing casein concentrations for both systems from pH 5.05 ± 0.01 to pH 4.89 ± 0.01. From this general trend, the calculated value of the pH at the tan δ_{max} could be described as a function of casein micelles concentration (g kg^{-1}) derived from the equation of Debye-Huckel:

$$\text{pH at the tan } \delta_{max} = A + \exp(-B * \text{square root } (C * \text{casein concentration})) \quad (7)$$

where A, B and C were constants, calculated by solver resolution that finds the optimal value of the constant. The increase in casein concentration in the NMC and MIX systems resulted in an increase in the ionic strength, hence in a decrease in the ionization of weak acids and in a small shift of CCP solubilization towards lower pH values (Famelart, Lepesant, Gaucheron, Le Graet, & Schuck, 1996).

3.2. pH of gelation of the model milk systems

Fig. 3A shows that the gels were formed at different pH values depending on the compositions of the model milk systems. When increasing from 15 to 70 g kg^{-1} protein, the pH of gelation of the WPA system increased from 5.47 to 5.82. When increasing from 45 to 105 g kg^{-1} protein, the pH of gelation of the MNC system increased from 4.97 to 5.53, while when increasing from 15 to 90 g kg^{-1} protein, the pH of gelation of the MIX system increased from 5.12 to 5.75. In all systems, the pH of gelation showed a linear correlation with the total protein concentration. This result was probably due to the increase in the number of particles and therefore, to the decrease of the inter-particle distance as the concentration increased. At all concentrations, the WPA-containing systems WPA and MIX both exhibited a significantly higher pH of gelation than the NMC system (Fig. 3A). In the current study, the apparent pI values of the WPA and NMC were found to be ~4.7 and ~4.4, respectively, which could partially explain the higher pH of gelation of WPA suspensions (Fig. 3B). These pI values were close to those found in other studies, namely 4.7 – 4.9 for whey protein aggregates (Jean, Renan, Famelart, & Guyomarc'h, 2006; Morand, Guyomarc'h, et al., 2012) and 4.2 - 4.6 for the casein micelles (Guyomarc'h et al., 2007; Lucey & Singh, 1998). Whey protein aggregates also have a higher surface hydrophobicity as compared to casein micelles (Guyomarc'h et al., 2007; Jean et al., 2006; Morand, Dekkari, et al., 2012), which can overcome electrostatic repulsion and induced stabilization of the system at higher pH values (Famelart et al., 2004; Morand, Dekkari, et al., 2012; Morand, Guyomarc'h, et al., 2012). As a complement, Fig. 3A also shows calculated values of the pH of gelation based on the respective proportions of NMC and WPA in the MIX systems. The calculated values were far below those measured in the MIX system, indicating a cooperative interaction between the two types of particles (Andoyo et al., 2014). In the MIX systems, the association of WPA particles with the surface of casein micelles occurs before the onset of gelation (Alexander &

Dalgleish, 2005; Donato, Alexander, & Dalgleish, 2007; Donato, Guyomarc'h, Amiot, & Dalgleish, 2007; Guyomarc'h, Jemin, Le Tilly, Madec, & Famelart, 2009) and these associated WPA are thought to cover the surface of the micelles and progressively replace the surface properties of micelles by their own (Morand, Dekkari, et al., 2012; Morand, Guyomarc'h, et al., 2012; Morand et al., 2011). As a result, the pH of gelation of systems was dramatically increased when 20% WPA were present, in agreement with Andoyo et al. (2014).

3.3. Rheological properties of the model milk systems at pH 4.5

The double-log plot of the G'_{max} of the gel as a function of the total protein concentration showed that increasing the protein concentration for the 3 systems led to higher G'_{max} values with a power law dependence (Fig. 3C), probably as a result of the increasing number of particles as discussed above. When increasing from 15 to 70 g kg^{-1} protein, the G'_{max} value of the WPA system increased from 1.06 x 10^2 to 1.09 x 10^5 Pa. When increasing from 45 to 105 g kg^{-1} protein, the G'_{max} value of the MNC system increased from 2.5 x 10^1 to 8.45 x 10^3 Pa, while when increasing from 15 to 90 g kg^{-1} protein, the G'_{max} value of the MIX system increased from 1.6 x 10^1 to 5.35 x 10^3 Pa. At 45 g kg^{-1} (log45=1.65), Fig. 3C also showed that the MIX system exhibited more than 43 times higher G'_{max} values than the NMC systems, in agreement with previous results (Andoyo et al., 2014). These authors explained that interaction of the WPA with the micelle surface led to the formation of earlier, more connected and stronger acid gels. However, Fig. 3C shows that such a significant effect of the presence of WPA in the MIX systems on the G'_{max} was only observed at protein concentration less than 90 g kg^{-1}(log 90=1.95). Indeed, the G'_{max} of the NMC systems increased with concentration at a higher rate than that of the MIX systems (Fig. 3C). This could be due to differences in the dimensions or density of the casein micelles or flocs of micelles in either

348 the NMC or the MIX systems, as evidenced by TEM micrographs (Fig. 5), as discussed
349 below.

350 When comparing the three different model milk systems, Fig. 3C furthermore shows that
351 the G'_{max} values of WPA systems were higher than those of the NMC or MIX systems at any
352 concentration. This could be due to the fact that heat-induced WPA are smaller and more
353 numerous than the casein micelles at any concentration (Andoyo et al., 2014), which increases
354 the number of contact points (bonds) between the particles forming the gel (Anema, 2008;
355 Van Vliet & Keetels, 1995). Heat-induced WPA also have higher surface hydrophobicity and
356 higher pI as compared to casein micelles, hence a higher reactivity to acid gelation and longer
357 time allowed for particle rearrangements until it reached pH 4.5 (Famelart et al., 2004).
358 However, the theoretical G'_{max} values, as calculated by combining 80% G'_{max} of NMC + 20%
359 G'_{max} of WPA, showed a lower values than the experimental G'_{max} (Fig. 3C). Therefore, the
360 interaction between WPA and the casein micelles in MIX systems synergistically increased
361 the final G'_{max}, as it increased the pH of gelation (Fig.3).

362 ***3.4. Arrangement of the particles, as interpreted using rheological measurements***

363 Fig. 4A, 4B and 4C show the double-logarithmic plots of the limit of linearity (γ_0) versus
364 the total protein concentration (C) of the WPA, NMC and MIX systems, respectively. The
365 $\gamma_0$data show a larger scatter than the data for G'. However, as the probability P to observe the
366 current values of the regression coefficient was <0.01 and as a regular distribution of the
367 residuals was found, a linear regression could significantly apply to log γ_0 versus log C.

368 According to Shih et al (1990), the sign of the slope (negative or positive) is indicative of
369 distinct aggregation pathways during flocculation. Furthermore, an apparent fractal dimension
370 (D_f) of the WPA, NMC and MIX systems can be directly calculated from the slope of the log
371 G' *versus* log C (Fig. 3C). The fractal dimension value expresses the volume occupancy by

the flocs: low D_f values correspond to a loose or diffuse flocs, while high D_f values correspond to compact flocs (Vetier et al., 1997). The present results show that for the WPA systems, γ_0 decreased with increasing particle concentration C. Meanwhile, γ_0 increased with C for both the NMC and MIX systems (Fig. 4B and 4C). For a negative slope, i.e. the WPA system, the value of the backbone fractal dimension of the flocs (x) has to be introduced. The range of the x value is 1 - 1.3 (Shih et al., 1990) and therefore, in this study a maximum and a minimum value of the apparent D_f were estimated using Eq. 1, respectively. Calculated D_f values for WPA model milk gel were 1.6 - 1.7 (Fig.3C). By using eqn.3 for a positive slope of log G' *versus* log C, the apparent D_f values of NMC and MIX systems were found to be 2.8 and 2.6, respectively (Fig. 3C). The values found for the casein gels (MNC and MIX) were higher than those found in previous studies on acid gels. Using light scattering measurement in diluted milk, D_f values of 1.85 – 2.44 were reported for acid casein gels (Bremer et al., 1989; Chardot, Banon, Misiuwianiec, & Hardy, 2002; Vetier et al., 1997). Values higher than 2.1 can occur when the repulsive barrier is high (Mellema, Walstra, Van Opheusden, & Van Vliet, 2002), as can occur with casein micelles. The apparent D_f values therefore indicated a more compact structure of the NMC and MIX gels than that of the WPA. On the other hand, the apparent D_f value for WPA gels was lower than those determined by Alting et al. (2003) for cold-set acid WPI gels, Hagiwara et al. (1996) for heat-set BSA gel or heat-set WPI gels by Ikeda et al. (1999) (1.6 against 2.0-2.3). This deviation could arise from different proteins and gelation processes used.

It is interesting to notice that when casein micelles were present, i.e. in NMC and MIX systems, a similar aggregation behavior was found, as indicated by the positive slopes of $\log \gamma_0$ with log C and by the similar D_f values, irrespective of the presence or absence of WPA. Meanwhile, it is clearly established that WPA, which do affect the final G' values of the gel (Andoyo et al., 2014; Guyomarc'h et al., 2003; Lucey & Singh, 1998), exhibited a

different aggregation behavior when gelled alone than when gelled in presence of the casein micelles, as shown by the negative slope of log γ_0 with log C for the WPA mixture and by the lower D_f values. The reason for this may lie in the scale of the particle assembly investigated by either approach. The G' value of a mature gel typically depends also on the strength and number of links established during percolation, while it was expected from Shih et al.'s approach to probe links established during the earlier fractal flocculation.

Gels that incorporate casein micelles, as the MNC and MIX systems, can rearrange upon acidification due to the dissolution of the CCP at pH ~ 5. This rearrangement can allow compaction of the protein clusters (Vetier et al., 1997), thus increasing the apparent D_f of the flocs (Mellema, Heesakkers, Van Opheusden, & Van Vliet, 2000) although this might be debated (Babu, Gimel, & Nicolai, 2008). When WPA are present in the MIX, stronger hydrophobic interactions and covalent bonds may lead to a higher stiffness of the links thus reducing the possibility for particles to rearrange in more compact flocs, hence the lower apparent D_f in MIX than in NMC. Furthermore, casein assemblies have a tendency to syneresis, especially in absence but even in presence of hydrophobic whey protein aggregates (Morand et al., 2011; Schorsch, Wilkins, Jones, & Norton, 2001). Contraction of the casein gel induces local rupture and opening of pores, while casein flocs densify. Inside the flocs, bonds between casein may become shorter, stronger and numerous as material came closer to each other, while those between flocs may be stressed, stretched and weaker or less numerous. WPA themselves are made of internal SS bonds (Hoffmann & Van Mil, 1997; Jean et al., 2006; Morand et al., 2011). When they are present along the casein micelles in the MIX system, the magnitude of the force, length and number of links are probably much higher than in their absence, i.e. in the NMC system (Andoyo et al., 2014; Lakemond & Van Vliet, 2008; Walstra & Jenness, 1984). When they are acidified alone, the WPA form clusters or flocs through non-covalent interactions (Hoffmann & Van Mil, 1997). Interactions may reorganize

through oxidation or SH/SS exchanges provided that the local environment is adequate, for example when high concentration of sulfhydryl and disulfides are locally present (Swaisgood, 2005; Guyomarc'h et al, 2014). Hence, it is suggested that it is the casein micelle fraction that actually drives the aggregation mechanism, while WPA would only affect bond strength and eventually G'. This is in line with the hypothesis that WPA particles modify the surface of the casein micelles, rendering them more prone to acid flocculation (Andoyo et al., 2014).

Microstructure of the gel at pH 4.5

Fig. 5 shows the TEM and CLSM images of acid gels of the 3 systems at pH ~4.5. In CLSM images (inserts in Fig. 5), the white color represented the protein network and black color represent the pores of the gel. From CSLM images, increasing the protein concentration of the system led to an increase in the whiteness of the image, i.e. to less pores. Images of the NMC and MIX gels seemed very close, although they are not shown at the same concentration. In the WPA systems, the gels were fully connected through the heat-induced whey protein aggregate network. Increasing total protein concentrations in the WPA systems yielded connected network, thus leading to smaller pores (Fig. 5A, B). The formation of smaller pores in the WPA gel as compared to NMC and mixture systems may indicate more numerous connections that led to a more homogeneous gel. Confocal images of the WPA gel, made from the 5 different protein concentrations, show that the structure of gels appeared finer and with smaller pores at higher protein concentration (inserts in Fig. 5AB). As we maintained the imaging parameters constant, we point out that images at higher protein concentrations had less contrast, probably due to the fact that the fluorescent probe is more homogeneously distributed in the matrix at a higher protein concentration, and because the pore size was more or less equal to the resolution of the microscope.

In the NMC systems, thick strands of gel can be seen on the images. TEM images in Fig. 5C showed that at low NMC concentration, the individual casein micelles particles still can be

447 seen. However, at a higher total protein concentration, the flocs of casein particles seemed to
448 enlarge (TEM Fig. 5D). The gels of NMC system at increased NMC concentrations show
449 smaller pore sizes, and denser, more clustered and less branched networks (insert Fig. 5C, D).
450 In the mixture systems, branched whey protein aggregates were slightly visible (TEM insert
451 Fig. 5A) and the casein micelles seemed intimately connected by whey protein aggregates
452 (TEM Fig. 5EF and insert Fig. 5F). When compared with the NMC system alone, the
453 association of heat-induced whey protein aggregates with casein micelles in the MIX system
454 largely changed the microstructure of the gels at pH ~4.5and at any concentration. First and
455 very significant, the size of the casein particles seemed to be much smaller as compared to the
456 size of the casein in the NMC systems as shown in the TEM micrograph (Fig. 5C, D, E, F).
457 Then the structure in the MIX gel appeared more branched and flocs were less dense and
458 more open than in the NMC gel. However, the changes of the gel microstructure at pH ~4.5 of
459 the MIX gel were not always correlated with changes in G' values, as the 2 gels 90 g kg^{-1}
460 protein did show differences in their microstructures but not on their G' values (Fig. 3B).

461 Apparent D_f values of each system were also calculated from confocal and TEM images
462 after binarization of the images. Average apparent D_f value for the 3 systems calculated with
463 the 2 image analysis methods and with the rheological measurements method are shown in
464 Fig. 6. The results showed a high standard deviation of the apparent D_f, measured from
465 confocal images, which can be due to the fact that slightly different threshold values were
466 applied on each concentration tested. Also, apparent D_f values of the WPA system could not
467 be determined from the TEM images, probably because the WPA flocs were smaller and less
468 contrasted than micelles one, so that no adequate thresholding could be operated.

469 Exclusive of the missing WPA value by TEM, apparent D_f values of 2.15, 2.76 and 2.74,
470 and 2.69 and 2.64 were found for the WPA, NMC and MIX systems, respectively, using the
471 TEM or the CLSM technique, respectively (Fig. 6). The apparent D_f values of the NMC and

MIX systems measured by image analysis agreed well with those obtained by the rheological method, the differences being lower than 5%. This indicates that image analysis is a good alternative method for the investigation of self-similarity within gels, providing that thresholding of the images is optimized using automated methods. Indeed, previous reports have shown that decreasing the grey scale thresholding parameter (i.e. increasing the number of pixels) can significantly increase the resulting D_f value (Ako, Durand, Nicolai, & Becu, 2009; Mellema et al., 2000).

3.6. Limits of the self-similarity approach for dairy gels

The concept of self-similarity has aroused a great interest in dairy science from the 80s onward, as it proposed a sensible description of protein flocculation or of fat crystallization (Alting et al., 2003; Bremer, Vanvliet, & Walstra, 1989b; Buscall et al., 1988; Hagiwara, Kumagai, Matsunaga, & Nakamura, 1997; Hagiwara et al., 1996; Marangoni et al., 2000; Mellema et al., 2000; Shih et al., 1990; Sonntag & Russel, 1987; Wu & Morbidelli, 2001). However, models are not without limitations.

Horne (1999) pointed out that fractal models fail to describe the macrostructure of acid gels of micellar casein, as they should yield gels with larger pores as the length scale increases. Alting et al. (2003) found that application of fractal models as proposed by Bremer et al. (1990) and Shih et al. (1990) to heat-induced WPI gels did not result in realistic values of the fractal dimension. They proposed that the gelation occurred with different mechanisms at certain length scales. In line with this, it could be assumed that a self-similar assembly only occurred in the suspensions at the early stages of the acid-induced aggregation, until the flocs started to come in contact, interpenetrate and eventually percolate into a gel. Therefore, the range of length scales where acid-induced self-similarity was investigated was ~0.1 to ~10 µm, using TEM and CLSM in the presented conditions. Noteworthy, the WPA particles are themselves short fractal aggregates (Jean et al., 2006; Mahmoudi, Mehalebi, Nicolai, Durand,

497 & Riaublanc, 2007), whereas the casein micelles are seen as hierarchical homogeneous
498 assemblies (Bouchoux, Gesan-Guiziou, Perez, & Cabane, 2010; de Kruif, Huppertz, Urban,
499 & Petukhov, 2012). Fractality may therefore exist in WPA-containing samples below the 0.1
500 µm length scale (Mahmoudi et al., 2007) and it is possible that the flocculation mechanism
501 somewhat differed from heat-induced to acid-induced aggregation.

502 According to computer simulation studies, the maximum volume fraction for which
503 fractality can be observed over a sensible scale range is 5% for DLCA and maybe 2-3 fold
504 that value for structures showing rearrangement (Babu et al., 2008; Rottereau, Gimel, Nicolai,
505 & Durand, 2004). This limitation was calculated for hard spheres and for diffusion-limited
506 cluster aggregations. Considering their mechanism, reaction-limited assemblies are
507 susceptible to tolerate even higher maximum volume fraction. According to Chaplain et al.
508 (1994), as micrographs of acid- or rennet-induced dairy gels show a typical persistent size in
509 chains of 10 particles, a limit close to 10% could be predicted for the maximal volume
510 fraction. By analogy with the polymers gels, these authors describe the gel structure at volume
511 fractions higher than the percolation threshold as a homogeneous packing of fractal flocs,
512 while a scaling behavior is only observed at short range. They developed a model adapted
513 from Bremer's, that leads to $\log(G') \sim \log(C)^3$ at high volume fraction, that leads to a Df of 3
514 i.e. a homogeneous gels made of fractal clusters. Our exponents of log (G') versus log (C)
515 were lower for gels studied in the current study (1.6-2.8). However, doubts exist on the
516 applicability of the fractal model to as high volume fractions as those used herein. Previous
517 groups also applied this theory to dairy systems with volume fractions in the range of those
518 used in the present study, using either rheometry or image analysis (Bremer et al., 1989;
519 Chaplain, Mills, & Djabourov, 1994; Hagiwara et al., 1997; Marangoni et al., 2000; Vetier,
520 Banon, Ramet, & Hardy, 2000; Zhong, Daubert, & Velev, 2004, 2007; Ikeda et al., 1999;
521 Pugnaloni et al., 2005; Torres et al., 2012). Many thermo-induced gels or flocs of whey

522 proteins at large volume fractions are also reported to be of fractal nature (Hagiwara,
523 Kumagai, & Matsunaga, 1997; Hagiwara, Kumagai, & Nakamura, 1998; Pouzot, Nicolai,
524 Benyahia, & Durand, 2006; Stading, Langton, & Hermansson, 1993; Verheul & Roefs, 1998).
525 In their study, Ako et al. (2009) investigated the structure of 100 g L^{-1} β-lactoglobulin heat-set
526 gels in 0.15-2 M NaCl, using CLSM and image analysis.

527 They found that the normalized pair correlation function g(r) did not show a power law
528 dependence on r that would be expected for a fractal structure. Instead, g(r) could be
529 described by a stretched exponential decay. Nevertheless, an apparent fractal dimension could
530 be derived using the box counting method. This finding raises the question of the validity of
531 the large number of studies that aimed at estimating fractal dimension in acid dairy gels at
532 concentrations > 15 g L^{-1}. Another interesting issue in this debate would be to agree on the
533 calculation of volume fraction of hydrated and porous particles like the casein micelles or the
534 WPA, which are not exactly hard spheres.

535 Another limitation of the self-similarity concept is that one should find a compromise
536 between extending the range of explored length scales through decreasing the protein
537 concentration (and hence, through postponing percolation) and having samples that can stand
538 rheological measurements or preparation for electron microscopy without breakage or phase
539 separation. Hence, if low volume fractions are required to apply the fractal model, one may be
540 limited by the sample itself. Mehalebi et al (2007) could observe heat-induced fractal
541 structures formed at high volume fraction, only after large dilution of the samples to disperse
542 the interpenetrating flocs.

543 Finally, a third limitation to the fractal theory is that one should assume that the particle
544 do not experience larger rearrangement than shifts in relative positions and may be slight
545 change in volume. Structural rearrangement occurred when casein micelles was present in the
546 systems, as evidenced by the local maximum of tan δ at pH ~5.0 (Fig.1D and 1F), which may

547 affect rheological measurements parameters such as G'_{max} and γ_0, therefore could implies to
548 the applicability of the fractal models.

549 In conclusion, the rheological properties and microstructure of 3 model systems, namely
550 NMC, WPA and MIX system, were investigated for a certain range of concentrations. Results
551 show that increasing the protein concentration for the 3 systems promoted a faster gelation,
552 led to higher moduli and to gels with smaller pore sizes, which is due to the increase in the
553 number of particles and consequently probably in the number of potential bonds between
554 them and to the reduction in the distances between colloids. Replacing 20 % of NMC by
555 WPA, as in MIX systems, increased the moduli of the acid gels as long as the protein
556 concentrations was < 90 g kg^{-1} and increased their pH of gelation as compared to pure NMC
557 gels. Although limitations existed, the model of Shih et al. (1990) indicated that the
558 aggregation behavior of the MIX system was similar to that of the NMC, and not of the WPA.
559 This result showed that the casein micelles directed the aggregation pathway wherever they
560 were present in the samples. On the other hand, WPA only seemed to impact on the amplitude
561 of the elastic modulus of the resulting gel, probably through affecting the strength of the
562 involved bonds. Further research is needed to be able to confirm these findings in conditions
563 where the scaling theory would fully apply.

564 **Acknowledgements**

565 We wish to thank MT LAVAULT from the Microscopy Rennes Imaging Center of SFR
566 BIOSIT, Université de Rennes 1 France for her expertise in TEM experiments. This work was
567 financially supported by the Directorate General of Higher Education (DGHE) of the Ministry
568 of Education and Culture of the Republic of Indonesia, as part of the DGHE scholarship
569 overseas program.

570 **References**

571 Ako, K., Durand, D., Nicolai, T., & Becu, L. (2009). Quantitative analysis of confocal laser
572 scanning microscopy images of heat-set globular protein gels. *Food Hydrocolloids*,
573 *23*(4), 1111–1119.

574 Alexander, M., Corredig, M., & Dalgleish, D. G. (2006). Diffusing wave spectroscopy of
575 gelling food systems: The importance of the photon transport mean free path (l*)
576 parameter. *Food Hydrocolloids*, *20*, 325–331.

577 Alexander, M., & Dalgleish, D. G. (2005). Interactions between denatured milk serum
578 proteins and casein micelles studied by diffusing wave spectroscopy. *Langmuir*,
579 *21*(24), 11380–11386.

580 Alting, A. C., Hamer, R. J., de Kruif, C. G., & Visschers, R. W. (2003). Cold-set globular
581 protein gels: interactions structure and rheology as a function of protein concentration.
582 *Journal of Agricultural and Food Chemistry*, *51*(10), 3150–3156.

583 Andoyo, R., Guyomarc'h, F., Cauty, C., & Famelart, M.-H. (2014). Model mixtures evidence
584 the respective roles of whey protein particles and casein micelles during acid gelation.
585 *Food Hydrocolloids*, *37*, 203–212.

586 Anema, S. (2009). Role of colloidal calcium phosphate in the acid gelation properties of
587 heated skim milk. *Food Chemistry*, 114, 161–167.

588 Anema, S. G. (2008). Effect of milk solids concentration on the gels formed by the
589 acidification of heated pH-adjusted skim milk. *Food Chemistry*, *108*(1), 110–118.

590 Awad, T. S., Rogers, M. A., & Marangoni, A. G. (2004). Scaling behavior of the elastic
591 modulus in colloidal networks of fat crystals. *The Journal of Physical Chemistry B*,
592 *108*(1), 171–179.

593 Babu, S., Gimel, J. C., & Nicolai, T. (2008). Diffusion limited cluster aggregation with
594 irreversible slippery bonds. *The European Physical Journal E*, *27*(3), 297–308.

595 Bertoluzzo, M. G., Bertoluzzo, S. M., Luisetti, J. A., & Gatti, C. A. (1998). A bidimensional
596 simulation of particle cluster aggregation with variable active sites particles. *Colloid*
597 *and Polymer Science*, *276*(5), 443–445.

598 Bi, C., Li, D., Wang, L., & Adhikari, B. (2013). Viscoelastic properties and fractal analysis of
599 acid-induced SPI gels at different ionic strength. *Carbohydrate Polymers*, *92*(1), 98–
600 105.

601 Bouchoux, A., Gesan-Guiziou, G., Perez, J., & Cabane, B. (2010). How to squeeze a sponge
602 casein micelles under osmotic stress, a SAXS study. *Biophysical Journal*, *99*(11),
603 3754–3762.

604 Bremer, L. G. B., Bijsterbosch, B. H., Schrijvers, R., Van Vliet, T., & Walstra, P. (1990). On
605 the fractal nature of the structure of acid casein gels. *Colloids and Surfaces*, *51*, 159–
606 170.

607 Bremer, L. G. B., Vanvliet, T., & Walstra, P. (1989a). Theoretical and experimental-study of
608 the fractal nature of the structure of casein gels. *Journal of the Chemical Society-*
609 *Faraday Transactions I*, *85*, 3359–3372.

610 Buscall, R., Mills, P., Goodwin, J., & Lawson, D. (1988). Scaling behavior of the rheology of
611 aggregate networks formed from colloidal particles. *Journal of the Chemical Society-*
612 *Faraday Transactions I*, *84*, 4249–4260.

613 Chaplain, V., Mills, P., & Djabourov, M. (1994). Elastic properties of networks of fractal
614 clusters. *Colloid and Polymer Science*, *272*(8), 991–999.

615 Chardot, V., Banon, S., Misiuwianiec, M., & Hardy, J. (2002). Growth kinetics and fractal
616 dimensions of casein particles during acidification. *Journal of Dairy Science*, *85*, 8–
617 14.

618 Dalgleish, D. G. (2011). On the structural models of bovine casein micelles-review and
619 possible improvements. *Soft Matter*, *7*(6), 2265–2272.

620 De Kruif, C. G. (1999). Casein micelle interactions. *International Dairy Journal*, *9*, 183–188.

621 De Kruif, C. G., Huppertz, T., Urban, V. S., & Petukhov, A. V. (2012). Casein micelles and
622 their internal structure. *Advances in Colloid and Interface Science*, *171*, 36–52.

623 De Kruif, C., & Huppertz, T. (2012). Casein micelles: size distribution in milks from
624 individual cows. *Journal of Agricultural and Food Chemistry*, *60*(18), 4649–4655.

625 Donato, L., Alexander, M., & Dalgleish, D. G. (2007). Acid gelation in heated and unheated
626 milks: interactions between serum protein complexes and the surfaces of casein
627 micelles. *Journal of Agricultural and Food Chemistry*, *55*(10), 4160–4168.

628 Donato, L., & Guyomarc'h, F. (2009). Formation and properties of the whey protein/κ-casein
629 complexes in heated skim milk - a review. *Dairy Science and Technology*, *89*, 3–29.

630 Donato, L., Guyomarc'h, F., Amiot, S., & Dalgleish, D. G. (2007). Formation of whey
631 protein/κ-casein complexes in heated milk: Preferential reaction of whey protein with
632 κ-casein in the casein micelles. *International Dairy Journal*, *17*(10), 1161–1167.

633 Dong, Y. J., Wang, Y. L., & Feng, J. (2011). Rheological and fractal characteristics of
634 unconditioned and conditioned water treatment residuals. *Water Research*, *45*(13),
635 3871–3882.

636 Eissa, A. S., & Khan, S. A. (2005). Acid-induced gelation of enzymatically modified,
637 preheated whey proteins. *Journal of Agricultural and Food Chemistry*, *53*(12), 5010–
638 5017.

639 Famelart, M. H., Lepesant, F., Gaucheron, F., Le Graet, Y., & Schuck, P. (1996). pH-Induced
640 physicochemical modifications of native phosphocaseinate suspensions: Influence of
641 aqueous phase. *Le Lait*, *76*, 445–460.

642 Famelart, M. H., Tomazewski, J., Piot, M., & Pezennec, S. (2004). Comprehensive study of
643 acid gelation of heated milk with model protein systems. *International Dairy Journal*,
644 *14*, 313–321.

645 Fox, P. F., & Brodkorb, A. (2008). The casein micelle: Historical aspects, current concepts
646 and significance. *International Dairy Journal*, *18*(7), 677–684.

647 Genovese, D. B. (2012). Shear rheology of hard-sphere, dispersed, and aggregated
648 suspensions, and filler-matrix composites. *Advances in Colloid and Interface Science*,
649 *171*, 1–16.

650 Guyomarc'h, F., Famelart, M.-H., Henry, G., Gulzar, M., Leonil, J., Hamon, P., Croguennec,
651 T. (2014). Current ways to modify the structure of whey proteins for specific
652 functionalities—a review. *Dairy Science & Technology*, 1–20.

653 Guyomarc'h, F., Jemin, M., Le Tilly, V., Madec, M. N., & Famelart, M. H. (2009). Role of
654 the heat-induced whey protein/κ-casein complexes in the formation of acid milk gels:
655 a kinetic study using rheology and confocal microscopy. The 5th International
656 Symposium on Food Rheology and Structure.

657 Guyomarc'h, F., Queguiner, C., Law, A. J. R., Horne, D. S., & Dalgleish, D. G. (2003). Role
658 of the soluble and micelle-bound heat-induced protein aggregates on network
659 formation in acid skim milk gels. *Journal of Agricultural and Food Chemistry*, *51*(26),
660 7743–7750.

661 Guyomarc'h, F., Renan, M., Chatriot, M., Gamerre, V., & Famelart, M. H. (2007). Acid
662 gelation properties of heated skim milk as a result of enzymatically induced changes

in the micelle/serum distribution of the whey protein/κ-casein aggregates. *Journal of Agricultural and Food Chemistry*, *55*(26), 10986–10993.

Hagiwara, T., Kumagai, H., & Matsunaga, T. (1997). Fractal analysis of the elasticity of BSA and β-lactoglobulin gels. *Journal of Agricultural and Food Chemistry*, *45*(10), 3807–3812.

Hagiwara, T., Kumagai, H., Matsunaga, T., & Nakamura, K. (1997). Analysis of aggregate structure in food protein gels with the concept of fractal. *Bioscience Biotechnology & Biochemistry*, *61*, 1663–1667.

Hagiwara, T., Kumagai, H., & Nakamura, K. (1996). Fractal analysis of aggregates formed by heating dilute BSA solutions using light scattering methods. *Bioscience Biotechnology and Biochemistry*, *60*(11), 1757–1763.

Hagiwara, T., Kumagai, H., & Nakamura, K. (1998). Fractal analysis of aggregates in heat-induced BSA gels. *Food Hydrocolloids*, *12*(1), 29–36.

Hoffmann, M. A. M., & Vanmil, P. J. J. M. (1997). Heat-induced aggregation of β-lactoglobulin: role of the free thiol group and disulfide bonds. *Journal of Agricultural and Food Chemistry*, *45*(8), 2942–2948.

Holt, C. (1992). Structure and stability of bovine casein micelle. *Advances in Protein Chemistry*, *43:63-151*, 63–151.

Horne, D. S. (1998). Casein interactions: casting light on the black boxes, the structure in dairy products. *International Dairy Journal*, *8*, 171–177.

Horne, D. S. (1999). Formation and structure of acidified milk gels. *International Dairy Journal*, *9*, 261–268.

685 Horne, D. S. (2001). Factors influencing acid-induced gelation of skim milk. In E. Dickinson
686 & R. Miller (Eds.), *Food colloids: fundamentals of formulation* (pp. 345–351).
687 Cambridge UK: Royal Society of Chemistry.

688 Ikeda, S., Foegeding, E. A., & Hagiwara, T. (1999). Rheological study on the fractal nature of
689 the protein gel structure. *Langmuir*, *15*(25), 8584–8589.

690 Jean, K., Renan, M., Famelart, M. H., & Guyomarc'h, F. (2006). Structure and surface
691 properties of the serum heat-induced protein aggregates isolated from heated skim
692 milk. *International Dairy Journal*, *16*, 303–315.

693 Kalab, M. (1981). Electron microscopy of milk products : A review of techniques. *Scanning*
694 *Electron Microscopy*, *3*, 453–472.

695 Kaye, B. H. (1994). *A random walk through fractal dimensions*. Weinheim; New York: VCH.

696 Kuhn, K. R., Cavallieri, Â. L. F., & Da Cunha, R. L. (2010). Cold-set whey protein gels
697 induced by calcium or sodium salt addition. *International Journal of Food Science &*
698 *Technology*, *45*(2), 348–357.

699 Lakemond, C. M. M., & Van Vliet, T. (2008). Rheological properties of acid skim milk gels
700 as affected by the spatial distribution of the structural elements and the interaction
701 forces between them. *International Dairy Journal*, *18*(5), 585–593.

702 Lucey, J. A. (2002). Formation and physical properties of milk protein gels. *Journal of Dairy*
703 *Science*, *85*, 281–294.

704 Lucey, J. A., & Singh, H. (1998). Formation and physical properties of acid milk gels: a
705 review. *Food Research International*, *30*(7), 529–542.

706 Mahmoudi, N., Mehalebi, S., Nicolai, T., Durand, D., & Riaublanc, A. (2007). Light-
707 scattering study of the structure of aggregates and gels formed by heat-denatured whey

protein isolate and β-lactoglobulin at neutral pH. *Journal of Agricultural and Food Chemistry*, *55*(8), 3104–3111.

Marangoni, A. G., Barbut, S., McGauley, S. E., Marcone, M., & Narine, S. S. (2000). On the structure of particulate gels - the case of salt-induced cold gelation of heat-denatured whey protein isolate. *Food Hydrocolloids*, *14*(1), 61–74.

Mellema, M., Heesakkers, J. W. M., Van Opheusden, J. H. J., & Van Vliet, T. (2000). Structure and scaling behavior of aging rennet-induced casein gels examined by confocal microscopy and permeametry. *Langmuir*, *16*(17), 6847–6854.

Mellema, M., Walstra, P., Van Opheusden, J. H. J., & Van Vliet, T. (2002). Effects of structural rearrangements on the rheology of rennet-induced casein particle gels. *Advances in Colloid and Interface Science*, *98*(1), 25–50.

Morand, M., Dekkari, A., Guyomarc'h, F., & Famelart, M. H. (2012). Increasing the hydrophobicity of the heat-induced whey protein complexes improves the acid gelation of skim milk. *International Dairy Journal*, *25*(2), 103–111.

Morand, M., Guyomarc'h, F., Legland, D., & Famelart, M. H. (2012). Changing the isoelectric point of the heat-induced whey protein complexes affects the acid gelation of skim milk. *International Dairy Journal*, *23*, 9–17.

Morand, M., Guyomarc'h, F., Pezennec, S., & Famelart, M. H. (2011). On how κ-casein affects the interactions between the heat-induced whey protein/κ-casein complexes and the casein micelles during the acid gelation of skim milk. *International Dairy Journal*, *21*, 670–678.

Nair, P. K., Dalgleish, D. G., & Corredig, M. (2013). Colloidal properties of concentrated heated milk. *Soft Matter*, *9*(14), 3815–3824.

731 Noebel, S., Weidendorfer, K., & Hinrichs, J. (2012). Apparent voluminosity of casein
732 micelles determined by rheometry. *Journal of Colloid and Interface Science*, *386*,
733 174–180.

734 Ozcan-Yilsay, T., Lee, W. J., Horne, D., & Lucey, J. A. (2007). Effect of trisodium citrate on
735 rheological and physical properties and microstructure of yogurt. *Journal of Dairy*
736 *Science*, *90*(4), 1644–1652.

737 Panouillé,, M., Durand, D., Nicolai, T., Larquet, E., & Boisset, N. (2005). Aggregation and
738 gelation of micellar casein particles. *Journal of Colloid and Interface Science*, *287*(1),
739 85–93.

740 Parris, N., Anama, S. G., Singh, H., & Creamer, L. K. (1993). Aggregation of whey proteins
741 in heated sweet whey. *Journal of Agricultural and Food Chemistry*, *41*(3), 460–464.

742 Parris, N., Hollar, C. M., Hsieh, A., & Cockley, K. D. (1997). Thermal stability of whey
743 protein concentrate mixtures: aggregates formation. *Journal of Dairy Science*, *80*, 19–
744 28.

745 Pawley, J. (2010). *Handbook of Biological Confocal Microscopy*. Springer Science &
746 Business Media.

747 Pouzot, M., Nicolai, T., Benyahia, L., & Durand, D. (2006). Strain hardening and fracture of
748 heat-set fractal globular protein gels. *Journal of Colloid and Interface Science*, *293*(2),
749 376–383.

750 Pugnaloni, L. A., Matia-Merino, L., & Dickinson, E. (2005). Microstructure of acid-induced
751 caseinate gels containing sucrose: Quantification from confocal microscopy and image
752 analysis. *Colloids and Surfaces B: Biointerfaces*, *42*(3-4), 211–217.

753 Rottereau, M., Gimel, J. C., Nicolai, T., & Durand, D. (2004). Monte Carlo simulation of
754 particle aggregation and gelation: II. Pair correlation function and structure factor.
755 *European Physical Journal E*, *15*(2), 141–148.

756 Schorsch, C., Wilkins, D. K., Jones, M. ., & Norton, I. T. (2001). Gelation of casein-whey
757 mixtures: effects of heating whey proteins alone or in the presence of casein micelles.
758 *Journal of Dairy Research*, *68*, 471–481.

759 Schuck, P., Piot, M., Mejean, S., Le Graet, Y., Fauquant, J., Brulé, G., & Maubois, J. L.
760 (1994). Déhydratation par atomisation de phosphocaséinate natif obtenu par
761 microfiltration sur membrane. *Le Lait*, *74*, 375-388.

762 Shih, W. H., Shih, W. Y., Kim, S. I., Liu, J., & Aksay, I. A. (1990). Scaling Behavior of the
763 Elastic Properties of Colloidal Gels. *Physical Review A*, *42*(8), 4772–4779.

764 Singh, H., & Creamer, L. K. (1991). Aggregation and dissociation of milk protein complexes
765 in heated reconstituted concentrated skim milks. *Journal of Food Science*, *56*, 238–
766 246.

767 Sonntag, R., & Russel, W. (1987). Elastic Properties of Flocculated Networks. *Journal of*
768 *Colloid and Interface Science*, *116*(2), 485–489.

769 Stading, M., Langton, M., & Hermansson, A. M. (1993). Microstructure and rheological
770 behavior of particulate β-lactoglobuline gels. *Food Hydrocolloids*, *7*, 195–212.

771 Swaisgood, H. E. (2005). The importance of disulfide bridging. *Biotechnology Advances*,
772 *23*(1), 71–73.

773 Torres, I. C., Amigo Rubio, J. M., & Ipsen, R. (2012). Using fractal image analysis to
774 characterize microstructure of low-fat stirred yoghurt manufactured with
775 microparticulated whey protein. *Journal of Food Engineering*, *109*(4), 721–729.

776 Van Hooydonk, A. C. M., Hagedoorn, H. G., & Boerrigter, I. J. (1986). pH-induced physico-
777 chemical changes of casein micelles in milk and their effect on renneting. 1. Effect of
778 acidification on physico-chemical properties. *Netherlands Milk and Dairy Journal*,
779 *40*(2/3), 281–296.

780 Van Vliet, T., & Keetels, C. J. A. M. (1995). Effect of preheating of milk on the structure of
781 acidified milk gels. *Netherlands Milk and Dairy Journal*, *49*, 27–35.

782 Van Vliet, T., Roefs, S. P. F. M., Zoon, P., & Walstra, P. (1989). Rheological properties of
783 casein gels. *Journal of Dairy Research*, *56*, 529–534.

784 Vasbinder, A. J., van de Velde, F., & de Kruif, C. G. (2004). Gelation of casein-whey protein
785 mixtures. *Journal of Dairy Science*, *87*, 1167–1176.

786 Verheul, M., & Roefs, S. P. F. M. (1998). Structure of whey protein gels, studied by
787 permeability, scanning electron microscopy and rheology. *Food Hydrocolloids*, *12*(1),
788 17–24.

789 Vetier, N., Banon, S., Ramet, J. P., & Hardy, J. (2000). Casein micelle solvation and fractal
790 structure of milk aggregates and gels. *Lait*, *80*(2), 237–246.

791 Vetier, N., Desobry-Banon, S., Ould-Eleya, M. M., & Hardy, J. (1997). Effect of temperature
792 and acification rate on the fractal dimension of acidified casein aggregates. *Journal of*
793 *Dairy Science*, *80*, 3131–3166.

794 Walstra, P., & Jenness, R. (1984). *Dairy chemistry and physics*. New York: John Wiley &
795 Sons.

796 Wang, Y., Lu, J., Du, B., Shi, B., & Wang, D. (2009). Fractal analysis of polyferric chloride-
797 humic acid (PFC-HA) flocs in different topological spaces. *Journal of Environmental*
798 *Sciences*, *21*(1), 41–48.

799 Wu, H., & Morbidelli, M. (2001). A Model Relating Structure of Colloidal Gels to Their
800 Elastic Properties. *Langmuir*, *17*(4), 1030–1036.

801 Zhong, Q., Daubert, C. R., & Velev, O. D. (2004). Cooling Effects on a Model Rennet Casein
802 Gel System: Part I. Rheological Characterization. *Langmuir*, *20*(18), 7399–7405.

803 Zhong, Q., Daubert, C. R., & Velev, O. D. (2007). Physicochemical variables affecting the
804 rheology and microstructure of rennet casein gels. *Journal of Agricultural and Food*
805 *Chemistry*, *55*(7), 2688–2697.

806

Figure caption

Fig. 1. Storage modulus (G') on a log scale and tan δ as a function of pH recorded during acidification at 35 °C of whey protein aggregates (WPA) systems (A and B), native micellar casein (NMC) systems (C and D) and the mixture (MIX) of 80% NMC and 20% of WPA systems (E and F) at different protein concentrations. In A-B, black is 13.42 g kg^{-1}, blue is 26.85 g kg^{-1}, purple is 40.27 g kg^{-1}, red is 53.69 g kg^{-1}, and green is 62.64 g kg^{-1}protein. In C-D, black is 42.16 g kg^{-1}, blue is 56.22 g kg^{-1}, purple 70.27 g kg^{-1}, red is 84.33 g $kg^{-1}$and green is 98.38 g kg^{-1}protein. in E-F, black is 13.92 g kg^{-1}, blue is 27.86 g kg^{-1}, purple is 41.78 g kg^{-1}, red is 55.71 g kg^{-1}, brown is 69.64 g $kg^{-1}$and green is 83.57 g kg^{-1} protein. Full and dashed lines in the same color indicate repetitions. Arrows indicate the direction of the protein concentrations increase.

Fig. 2. pH at tan δ_{max} as a function of casein concentration in native micellar casein (NMC) systems (o) and in the in the mixture system (MIX) of 80% NMC and 20% of WPA(●). The line drawn is of the form of the equation of Debye Huckel.

Fig. 3. pH of gelation of whey protein aggregates (WPA) systems (O), native micellar casein (NMC) systems (◊) and mixture (MIX) systems (△) at different protein concentrations (A), electrophoretic mobility of WPA (O) and NMC (◊) (B) and double log storage modulus at pH 4.5, G'_{max} as a function of protein concentration (C) of WPA systems (O), NMC systems (◊) and MIX systems (△). Vertical bars indicate the standard deviation. The theoretical values of G'_{max} and pH of gelation for the mixture systems were calculated by using the content in each protein and their own G' and pH of gelation, respectively (■). D_f is the fractal dimension value of each system, calculated from the slope of double-log G'_{max} versus C.

Fig. 4. Log-log plot of the limit of linearity (γ) versus the protein concentration (C) of the WPA systems (A), NMC system (B) and MIX systems (C). Inserted in panel B is an example

of estimation of the limit of linearity (γ_0) from shear stress - strain curve of the model system. The linear regression is drawn to show γ_0 value as the strain above which the slope of the stress versus strain curve decreased of 5% from its maximal value.

Fig. 5. Transmission electron micrographs and confocal images of gels from the three different systems and at two different total protein concentrations: WPA (A, B); NMC (C, D); MIX (E, F); low concentration (A, C, E) and high concentration (B, D, F).TEM at higher magnification (inserts B, F).

Fig. 6. Fractal dimension (D_f) of the different systems measured with different methods. Vertical bars represent the standard deviation from images analyzed at different concentrations.

1 **Table captions**

2 **Table 1**

3 Composition of the model milk protein systems and GDL concentrations used to reach pH 4.5
4 in 6 h at 35°C. The 3 systems are the native micellar casein system (NMC), the whey protein
5 aggregate system (WPA) and the mixture system (MIX) of 80% NMC and 20% of WPA.

Model system	Casein ($g\ kg^{-1}$)	Whey proteins ($g\ kg^{-1}$)	Total protein concentration ($g\ kg^{-1}$)	GDL Conc. ($g\ kg^{-1}$)
WPA15	-	13.42	13.42	5.84
WPA30	-	26.85	26.85	7.69
WPA45	-	40.27	40.27	9.54
WPA60	-	53.69	53.69	11.39
WPA70	-	62.64	62.64	12.63
NMC45	42.16	-	42.16	18.74
NMC60	56.22	-	56.22	23.06
NMC75	70.27	-	70.27	27.39
NMC90	84.33	-	84.33	31.71
NMC105	98.38	-	98.38	36.03
MIX15	11.24	2.68	13.92	8.71
MIX30	22.49	5.37	27.86	12.55
MIX45	33.73	8.05	41.78	16.39
MIX60	44.97	10.74	55.71	20.23
MIX75	56.22	13.42	69.64	24.06
MIX90	67.46	16.11	83.57	27.90

6

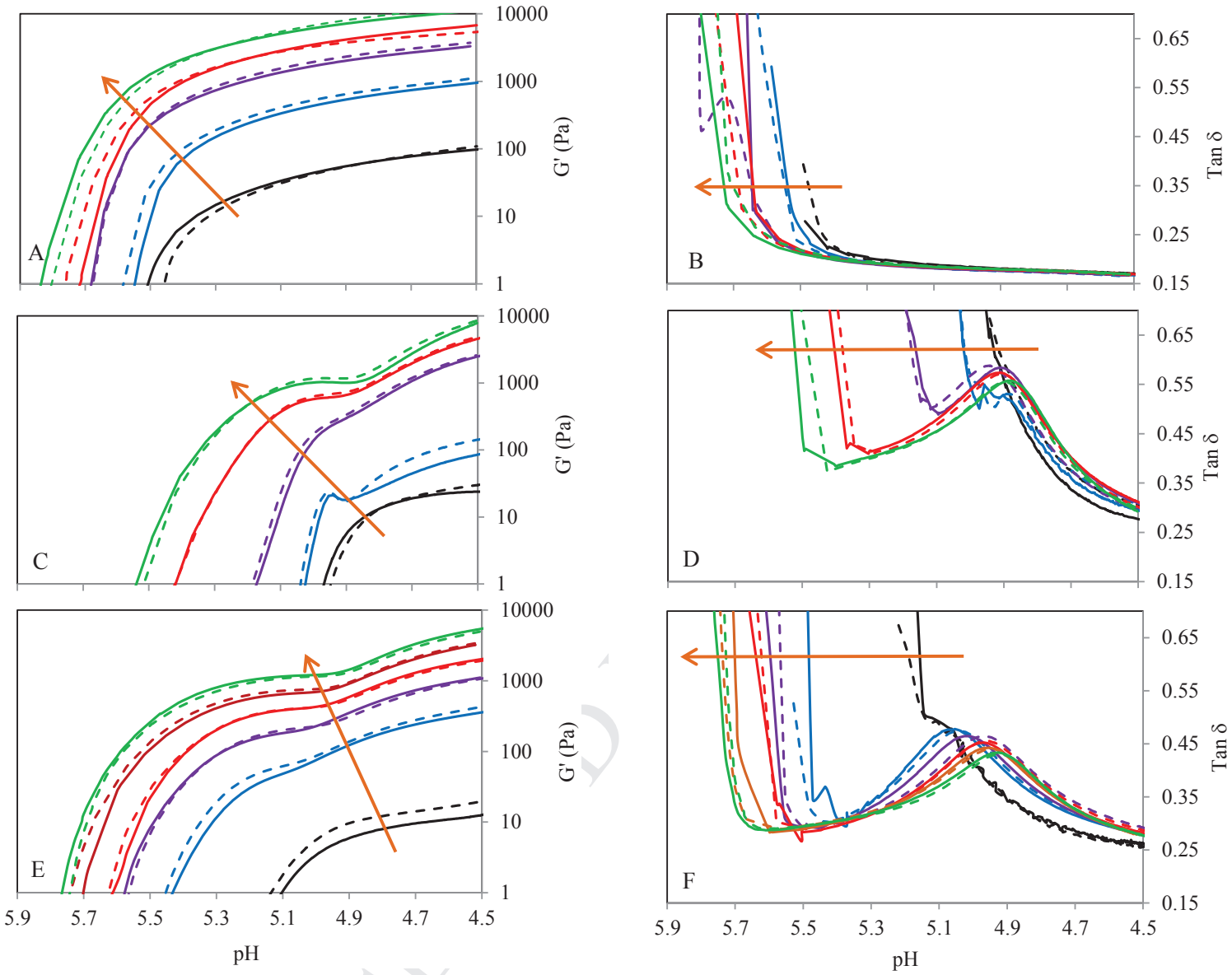
A
B
C
D
E
F
10000
1000
100
10
1
G' (Pa)
0.65
0.55
0.45
0.35
0.25
0.15
Tan δ
5.9
5.7
5.5
5.3
5.1
4.9
4.7
4.5
pH

Fig. 1.

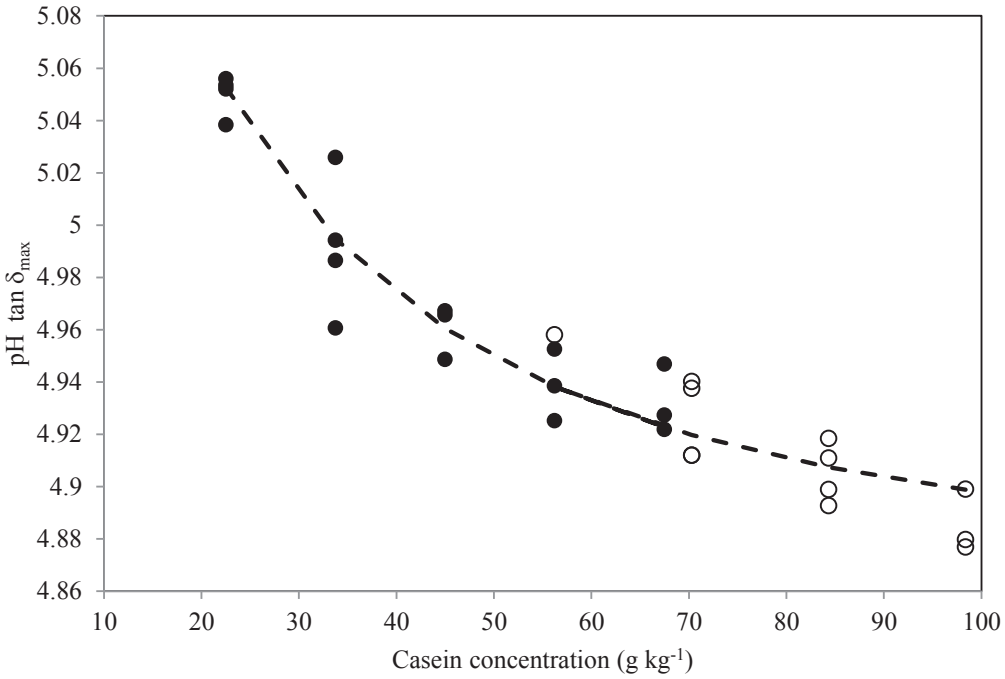

Fig. 2.

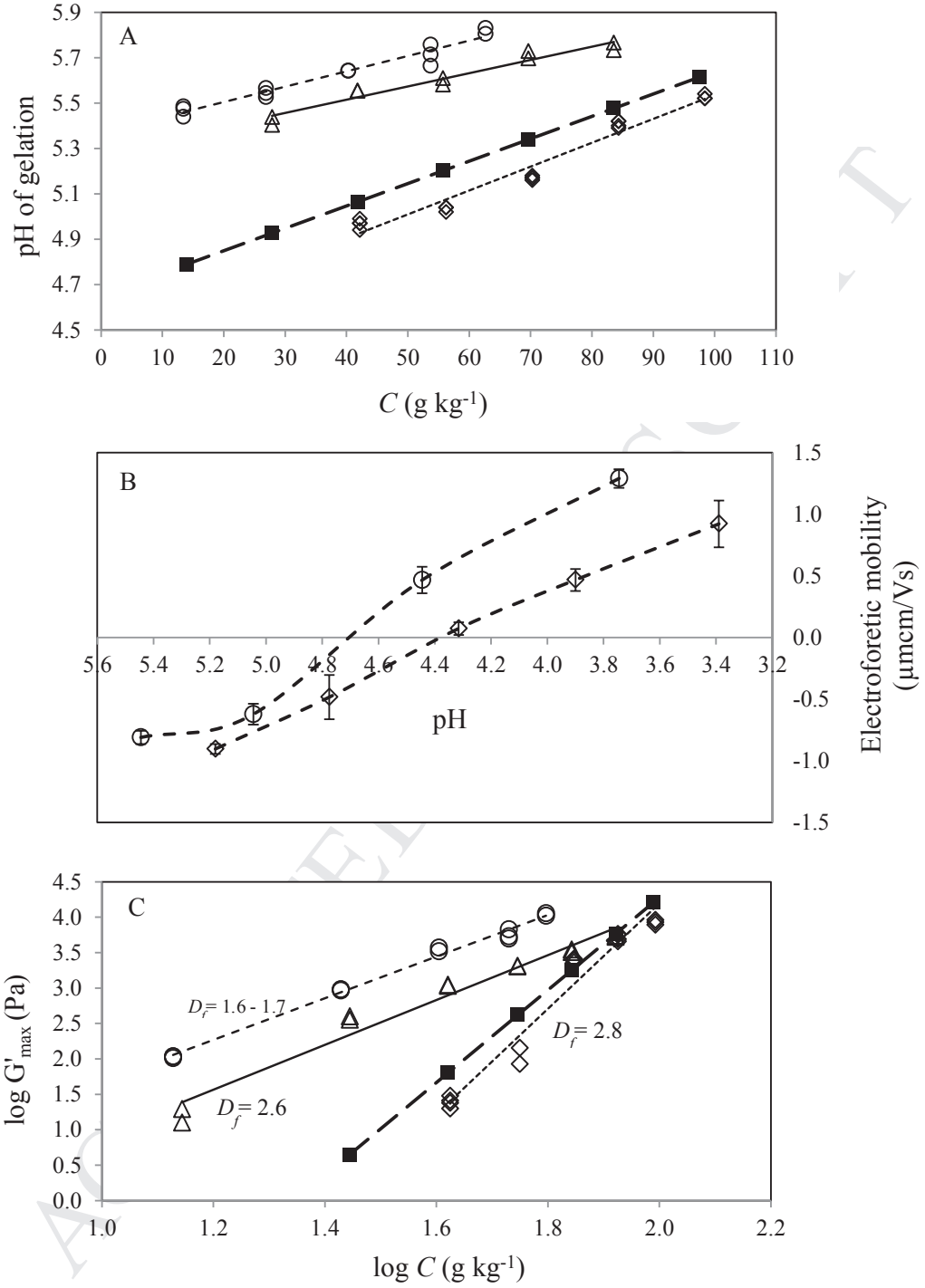
A
pH of gelation
5.9
5.7
5.5
5.3
5.1
4.9
4.7
4.5
0
10
20
30
40
50
60
70
80
90
100
110
C (g kg-1)
B
1.5
1.0
0.5
0.0
-0.5
-1.0
-1.5
5.6
5.4
5.2
5.0
4.8
4.6
4.4
4.2
4.0
3.8
3.6
3.4
3.2
pH
Electroforetic mobility (μmcm/Vs)
C
log G'max (Pa)
4.5
4.0
3.5
3.0
2.5
2.0
1.5
1.0
0.5
0.0
1.0
1.2
1.4
1.6
1.8
2.0
2.2
log C (g kg-1)
Df= 1.6 - 1.7
Df= 2.6
Df= 2.8

Fig. 3.

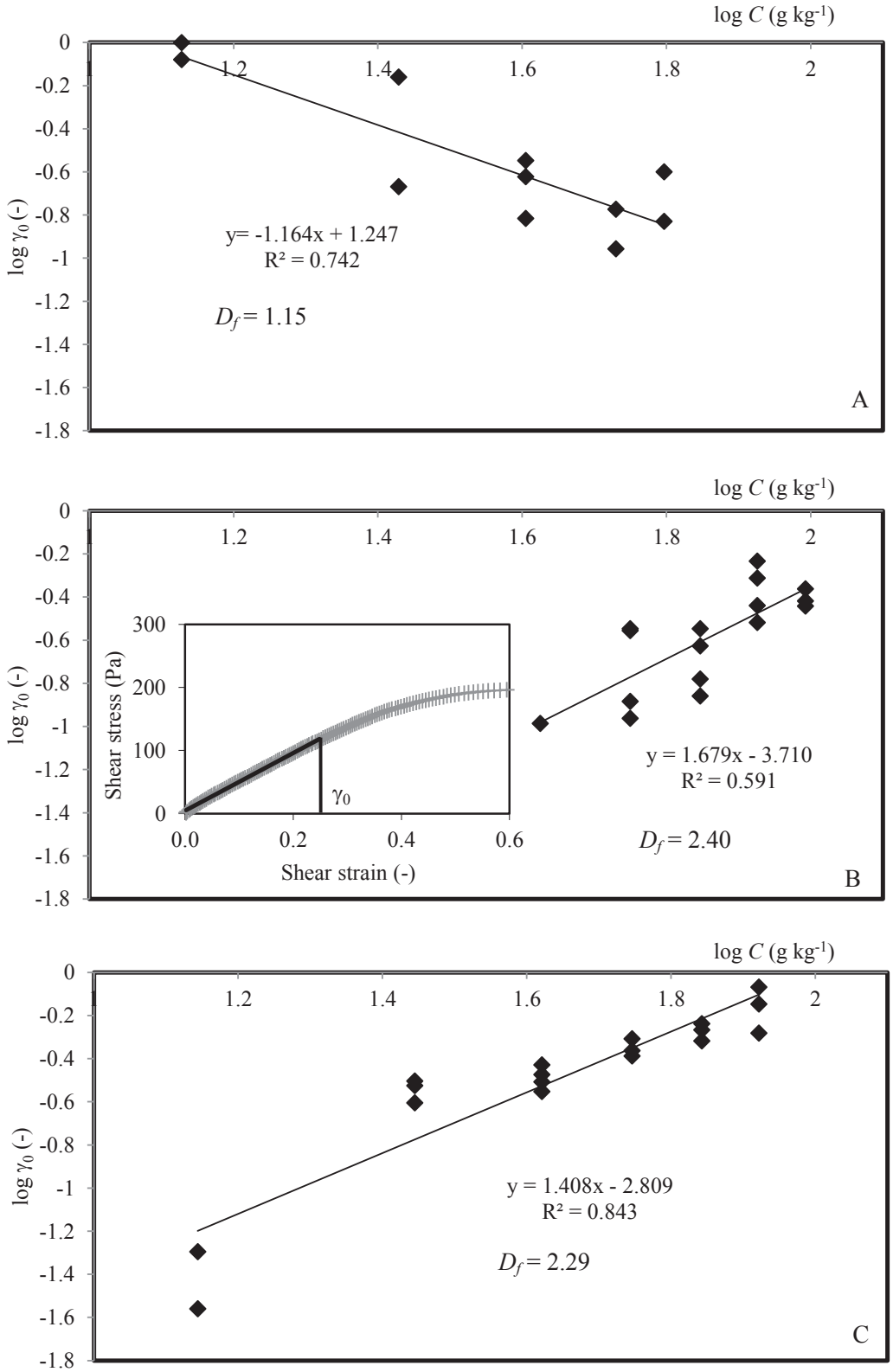
log C (g kg-1)
log γ0 (-)
y= -1.164x + 1.247
R² = 0.742
Df = 1.15
A
log C (g kg-1)
log γ0 (-)
Shear stress (Pa)
Shear strain (-)
γ0
y = 1.679x - 3.710
R² = 0.591
Df = 2.40
B
log C (g kg-1)
log γ0 (-)
y = 1.408x - 2.809
R² = 0.843
Df = 2.29
C

Fig. 4.

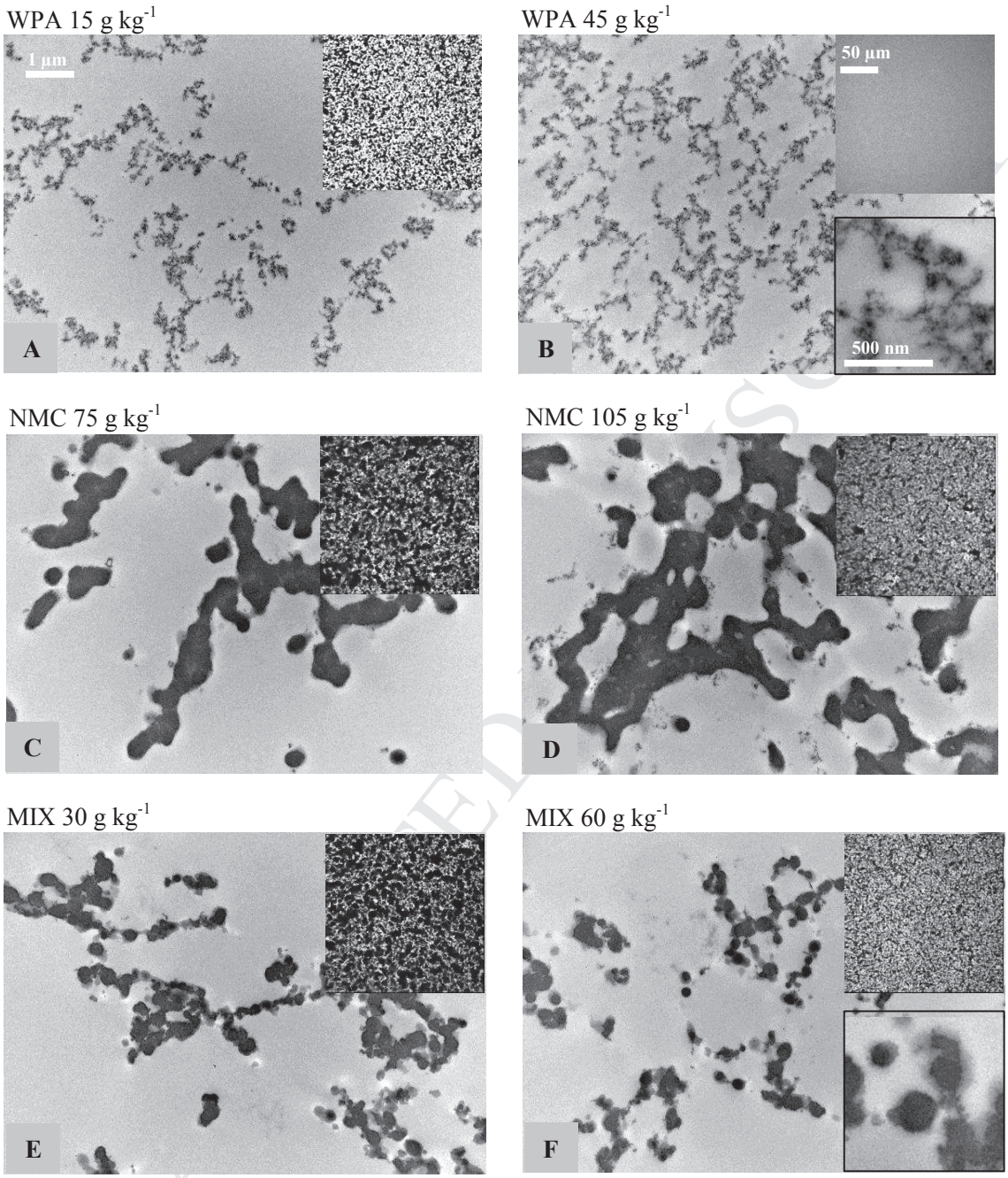
WPA 15 g kg-1
1 µm
A
WPA 45 g kg-1
50 µm
500 nm
B
NMC 75 g kg-1
C
NMC 105 g kg-1
D
MIX 30 g kg-1
E
MIX 60 g kg-1
F

Fig. 5.

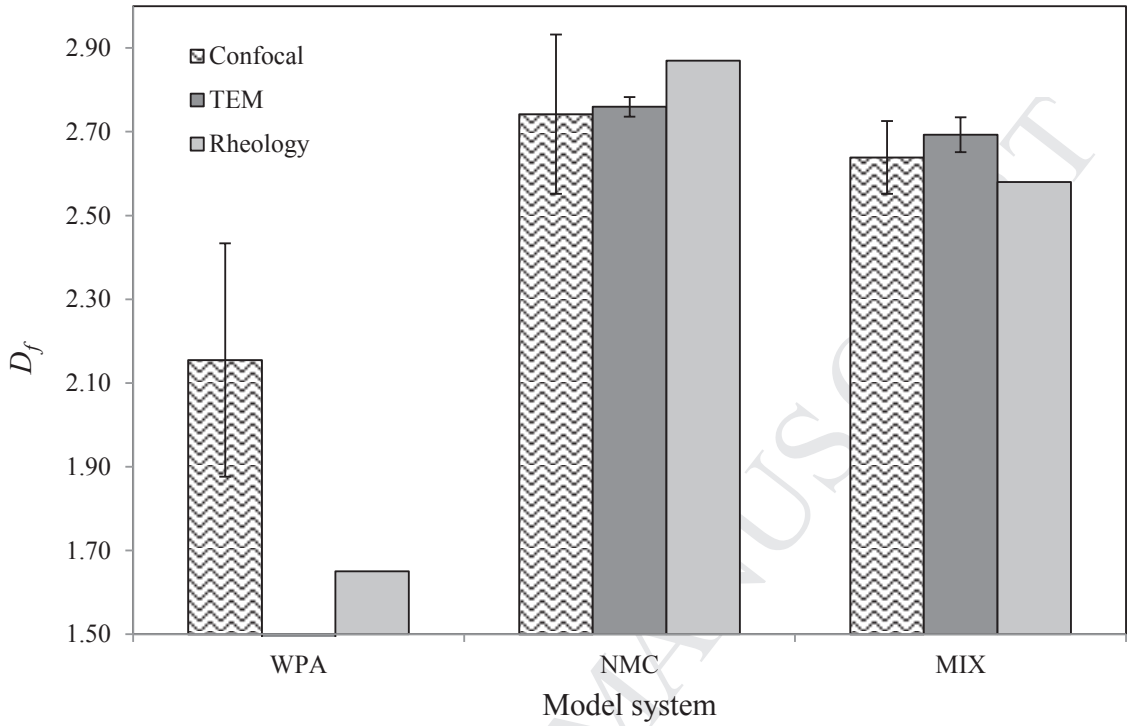

Fig. 6.

Highlights

- Acid gels were made from casein micelles (NMC) and whey protein aggregates (WPA)
- Acid gels were made from 80/20 mixtures of NMC and WPA, respectively
- Fractal dimension (D_f) of gel flocs were determined by rheology and image analysis
- Replacement of 20% NMC by WPA hardly changes the D_f value of the flocs
- Aggregation in the NMC and MIX mixtures was driven by the casein micelles